PROCEEDINGS, Eleventh Workshop on Geothermal Reservoir Engineering
Stanford University, Stanford, California, January 21-23, 1986
SGP-TR-93

A FIELD STUDY OF TRACER AND GEOCHEMISTRY BEHAVIOR DURING HYDRAULIC FRACTURING OF A HOT DRY ROCK GEOTHERMAL RESERVOIR

Bruce A. Robinson

Earth and Space Sciences Division
Los Alamos National Laboratory
Los Alamos, NM 87545

ABSTRACT

Tracer and geochemistry measurements in fractured Hot Dry Rock (HDR) geothermal reservoirs are usually performed after a fracture connection has been established and constant, nearly equal inlet and outlet flow rates have been achieved. However, during hydraulic fracturing experiments designed to create a low-impedance fracture connection between two wells, the inlet and outlet flow rates can be dramatically different and can vary during the test, forcing us to revise the common analytical methods for interpreting tracer response curves and geochemistry behavior.

This study presents tracer and geochemistry data from several hydraulic fracturing experiments at the Fenton Hill, NM, HDR geothermal reservoir. Tracers have been injected at various times during these tests: 1) initially, before any flow communication existed between the wells; 2) shortly after a flow connection was established; and 3) after the outlet flow had increased to its steady state value. An idealized flow model consisting of a combination of main fracture flow paths and fluid leakoff into secondary permeability explains the different tracer response curves for these cases, and allows us to predict the fracture volume of the main paths.

The geochemistry during these experiments supports our previously developed models postulating the existence of a high concentration indigenous "pore fluid." Also, the quartz and Na-K-Ca geothermometers have been used successfully to identify the temperatures and depths at which fluid traveled while in the reservoir. The quartz geothermometer is somewhat more reliable because at these high temperatures (about 250°C) the injected fluid can come to equilibrium with quartz in the reservoir. The Na-K-Ca geothermometer relies on obtaining a sample of the indigenous pore fluid, and thus is somewhat susceptible to problems of dilution with the injection fluid.

INTRODUCTION AND BACKGROUND

The hot dry rock geothermal concept currently being developed at the Fenton Hill, NM and Rosemanowes Quarry, Cornwall UK geothermal sites consists of creating a network of high-permeability fractures between two wellbores drilled into hot granite or crystalline basement rock of low inherent permeability (see Figure 1). Water is circulated down one wellbore, through the large volume of hot rock defined by the fracture network, and is collected and brought to the surface as heated, pressurized water to be utilized for electricity generation. The creation and characterization of the downhole fracture network of the Fenton Hill reservoir has been the goal of the Los Alamos HDR project for the past three years. The role of tracers and geochemistry in this effort is reported in the present study.

In previous HDR reservoir studies, tracers and geochemistry have been used extensively in systems which have already been created and steady state circulation established (Tester et al., 1982, Grigsby, 1983, Robinson and Tester, 1984). Tracers are used to measure the fracture volume of both main and secondary flow paths and to estimate the flow split among fractures of various permeabilities (Robinson and Tester, 1984). The tracer modal volume V, the produced fluid volume corresponding to the peak of the tracer response curve, is a good measure of the fracture void volume of the main flow paths. In previously operated reservoirs in which tracer and long-term energy extraction measurements have been made, V can be correlated roughly with the effective heat transfer surface area as determined from produced fluid temperature decline over time. Figure 2 illustrates this correlation. The effective heat transfer surface area is the area of a single fracture which would result in the measured rate of produced fluid cooldown, and thus is obviously a simplification. Nonetheless, the correlation implies that a single measurement of fracture volume using tracers can provide an estimate, subject to uncertainties, of the heat

transfer capacity of an HDR reservoir. Geochemical behavior in these circulating systems can be treated with analytical techniques similar to those of tracer studies. Grigsby (1984) has outlined the theory necessary to evaluate experiments in which the geochemical content of the injected fluid is changed temporarily. The quartz and Na-K-Ca geothermometers have also been used in reservoir evaluation.

Unfortunately, during the hydraulic fracturing of an HDR reservoir, the interpretation of tracer and geochemistry data is much more complex and subject to uncertainty. In the fracturing experiments described below, little or no hydraulic communication existed when pumping began. As a test proceeded, the outlet flow rate increased, and the ratio of fluid produced to fluid stored in the fracture system decreased. Thus the timing of the tracer injection and the inlet and outlet fluid flow rates affect the tracer response in a manner unlike that experienced in the steady state tests. Geochemistry is difficult to interpret as a tracer in these experiments, but the geothermometers are actually more useful in these transient tests for determining temperatures and depths at which fluid is being produced. Fracturing experiments of the so-called Phase II reservoir at Fenton Hill are described below, and tracer and geochemical techniques are developed to evaluate the reservoir fracture system.

THE FENTON HILL PHASE II CAMPAIGN

The Phase II campaign at the Fenton Hill geothermal site is designed to demonstrate the commercial feasibility of the HDR geothermal energy concept. The first reservoirs proved the technical merits of the concept, but the reservoir lifetimes and thermal energy production levels were too small in these prototype systems to be commercially interesting. Figure 3 provides a useful reference for the following description of events. In August 1982, two new wellbores (EE-2 and EE-3) were drilled to a depth of about 3.9 km, with the final 1.4 km inclined at an angle up to 35° from vertical. Several hydraulic fracturing experiments were performed in both wells without achieving the desired flow communication between EE-2 and EE-3. The most important of these was Experiment 2032, in which a total of 21000 m^3 of water was injected in EE-2 at an average flow rate of 0.1 m^3/sec and 48 MPa surface pressure. House et al. (1985) presented an analysis of the microseismic events located during this fracturing experiment, and one perspective of these events are shown in Figure 3.

As evidenced by the seismicity, the injected fluid stimulated a series of fractures which were essentially parallel to the two wellbores, and thus the intersection of the two holes with a network of flowpaths was not possible with this wellbore/fracture geometric configuration. Thus it was decided to redrill the bottom portion of wellbore EE-3 to intersect the 3-dimensional "cloud" of microseismicity located during Experiment 2032. Figure 3 also shows the nearly vertical trajectory of the new section of wellbore called EE-3A.

This redrilling was interrupted and followed by several hydraulic pressurization experiments in the new EE-3A wellbore, two of which were successful in creating the desired fracture flow communication between the two holes. Hydraulic fracturing is almost certainly a misnomer here, as the pumping most likely resulted in restimulation of the existing flowpaths created during Experiment 2032 described above. However, after several years of fluid diffusion away from this stimulated zone, the joints required more pressurization to increase their hydraulic conductivity. This was done using a newly designed openhole packer, which allowed specific intervals of wellbore EE-3A to be pressurized independently. Another essential reason for the openhole packer is the existence in the openhole region at 3.1 km (10250 ft) of a high-permeability zone which accepts large amounts of fluid at low pressures. This zone is not connected to EE-2, and eliminates any attempt to pump fluid into the formation at lower depths without a packer.

There are four packer flow stimulation tests for which there are tracer and/or geochemistry data of interest. Experiment 2032, the massive hydraulic fracturing experiment in wellbore EE-2, was described earlier. Experiment 2059 was the first successful attempt in the Phase II reservoir to achieve hydraulic communication between the wells. It was performed with the packer set at a relatively shallow depth in EE-3A. A second stimulation test, Experiment 2061, pressurized a region much deeper in the wellbore, with a much greater separation distance between the injection and target production regions. In this instance hydraulic communication was not established. Finally, Experiment 2062 created a second set of flow paths connecting the wells. The packer was set at an intermediate depth, and after 8 hours of pumping, interwell flow was achieved.

TRACER DATA ANALYSIS

The primary goal of HDR reservoir modeling is to estimate the reservoir heat transfer capacity and thus the potential lifetime of the system. The tracer modal volume $\bar{V}$ has been shown to be useful in this regard when steady state circulation experiments are

performed (Figure 2). Since this volume is best thought of as the fracture volume associated with the main fracture flow paths, this correlation is not surprising: the most direct hydraulic connections are likely to cool most rapidly, and thus control the heat transfer capacity.

When tracer experiments are carried out during the pumping experiments described below, the inlet flow rate was larger than the outlet rate as the hydraulic connection was developed. This net accumulation of water in the reservoir must be accounted for to calculate the volume of the main fracture flow paths. This situation is depicted schematically in Figure 4, which assumes interwell flow through the main joints and fluid leakoff into secondary permeability. Tracer travels through the main fractures most rapidly near the inlet and slows down due to water leakoff with distance or volume until it is traveling at the production flow rate when it leaves the system. The unknown is the main fracture volume (assumed to be the tracer modal volume V), which is found from the following integration:

$$\overset{\circ}{\tau} = \int_0^{\overset{\circ}{V}} \frac{dV}{Q} \qquad (1)$$

$\overset{\circ}{\tau}$ is the measured modal residence time and the independent variable V is the fractional volume of the main paths (0 at the entrance and V at the exit). An expression for $Q = Q(V)$ is needed to derive an analytical expression for V. The simplest possible relation is obtained by assuming a linear decline in flow rate with V, or

$$Q = Q_{in} - \frac{(Q_{in}-Q_{out})V}{\overset{\circ}{V}} \qquad (2)$$

Substituting Eqn. (2) into (1), we obtain, after integration and rearrangement:

$$\overset{\circ}{V} = \frac{\overset{\circ}{\tau}(Q_{in}-Q_{out})}{\ln\left(\frac{Q_{in}}{Q_{out}}\right)} \qquad (3)$$

Perhaps a more realistic representation of the flow rate is obtained by assuming a linear pressure decline along the main fractures, implying that the fractional water loss linearly decreases. Assuming no water loss to the formation at V=V, the appropriate expression for the flow rate for this model is

$$Q = Q_{in} - 2(Q_{out}-Q_{in})\left(\frac{1}{2}\left[\frac{V}{\overset{\circ}{V}}\right]^2 - \frac{V}{\overset{\circ}{V}}\right) \qquad (4)$$

When Eqn. (4) is substituted into Eqn. (1), the resulting expression for V is

$$\overset{\circ}{V} = \frac{-\overset{\circ}{\tau}\, Q_{out}(Q_{in}-Q_{out})}{\tan^{-1}\left(-\sqrt{\frac{Q_{in}-Q_{out}}{Q_{out}}}\right)} \qquad (5)$$

Equations (3) and (5) will be used to evaluate two of the tracer experiments below.

Experiment 2059: This experiment was the first fracturing test in the Phase II reservoir which resulted in a successful connection between the wells. To prove that the vent fluid at EF-2 was indeed caused by fluid injected at EE-3, 1 kg of sodium fluorescein dye was placed in the injection well before pumping began. Colorimetric measurements of the produced fluid using a UV-visible spectophotometer verified the presence of the dye. Unfortunately, the strategy of placing the tracer in the well before pumping began made the extraction of quantitative information about the reservoir nearly impossible. After the production well had vented the entire wellbore volume, tracer immediately appeared in the fluid, suggesting that the tracer front had traversed the entire wellbore separation distance before venting began. Given this situation, it is difficult to estimate the tracer transit time $\overset{\circ}{\tau}$ to use in Eqns. (3) and (5).

The only reliable quantitative information from this tracer test is the total mass of tracer collected during the vent. In this test 32% of the tracer injected into EE-3 was collected at EE-2, compared to an expected maximum of 47%, which is the ratio of the water volume vented to the amount injected. This recovery (68% of the expected maximum) seems quite high, especially since the reservoir was not a closed, confined system with limited boundaries during the test. Thus the data suggest that a short-circuiting flow path probably exists between the wells, allowing most of the injected tracer to reach the production wellbore rapidly. Since a commercially viable hot dry rock reservoir requires a sweep of fluid through a large rock volume, this direct interwell connection is not an acceptable result, and further hydraulic fracturing experiments were carried out.

Experiment 2062: This test was the second successful attempt to connect wellbores EE-3 and EE-2 with a set of hydraulically stimulated fractures, this time with the injection region at a depth about 150 m deeper in EE-3A. The difficulties in quantitatively analyzing the data of the previous tracer test led to changes in the tracer interrogation strategy for this experiment, with significantly improved results. The foremost rule learned from Experiment 2059 was that tracer should be injected only after a hydraulic connection is achieved. Also, during the tracer test the inlet and outlet flow rates should be kept as constant as possible to minimize unwanted

transients. Two tracer experiments were performed during Experiment 2062. The first was a 0.91 kg (2 lb) sodium fluorescein dye pulse injected early after the production vent began. In the second experiment, after the inlet and outlet flow rates were more nearly equal, three tracers were injected: 0.91 kg (2 lb) sodium fluorescein dye, 113.6 kg (250 lb) sodium bromide, NaBr, and 22.7 kg (50 lb) sodium nitrate, $NaNO_3$. The NaBr and $NaNO_3$ were analyzed for Br^- and NO_3^-, respectively, using an anion chromatograph. Figures 5 and 6 show the tracer responses for these two experiments, with the ordinate corrected for background levels and wellbore residence times, and the concentration is normalized so that the area under the curve would be unity for complete recovery of all injected tracer. Figure 5 compares the normalized response curves for the three tracers injected in the second experiment. Since the peak response for all three tracers occurred simultaneously, all tracers are non-adsorbing to within the limit of measurability. The differences in response curves are most likely due to measurement difficulties at high concentration in the case of the dye, and possible degradation of NO_3^- for the nitrate. Nonetheless, the modal volume V can be accurately determined: based on the produced fluid volume, V is 260 $\pm$20 m^3.

Figure 6 compares the dye tracer responses for the two tracer tests in Experiment 2062. The discrepancy in peak response volumes can be explained using the conceptual reservoir models described earlier. The first test was operated at higher injection and lower outlet flow rate. Using Eqns. (3) and (5) the modal volume estimates for the two experiments are:

Experiment 1:	550 m^3	Eqn. (3)
	371 m^3	Eqn. (5)
Experiment 2:	470 m^3	Eqn. (3)
	388 m^3	Eqn. (5)

For either of the models, the calculated values of V for the two tracer tests agree adequately. However, the choice of the model affects the result, making it difficult to assign a precise value to V. In round numbers, 400 m^3 is our best estimate for modal volume for Experiment 2062. As seen in Figure 2, this volume is larger than that of any fracture system previously created at Fenton Hill. Consequently the reservoir lifetime should be correspondingly higher. Future operations will attempt to enlarge the reservoir still more and increase the hydraulic conductivity between the wells.

GEOCHEMISTRY RESULTS

Geochemistry in the Fenton Hill reservoir is controlled by both active dissolution of minerals and displacement of indigenous pore fluid. In the steady state operational mode, injection of fresh water low in concentration of dissolved ions results in behavior quite similar to an interwell tracer. However, during a hydraulic fracturing experiment, transient effects dominate the early geochemical behavior. When a pressurized, shut-in production well is first opened, a rush of almost pure pore fluid enters the wellbore. As time proceeds and the interwell connection improves, the pore fluid becomes more and more diluted with injection fluid until constant concentrations are reached. This situation, though simple to describe qualitatively, does not provide much information about fracture volume or dispersive characteristics.

Despite this fact, geochemistry in the form of chemical geothermometers provides valuable information about the fluid temperature and hence depth when it resided in the reservoir. This temperature, combined with a background temperature log, yields the depth at which fluid traveled in the fracture system. The two most effective geothermometers for the Fenton Hill HDR reservoirs are the quartz and Na-K-Ca geothermometers, although their application is somewhat different due to the difference in equilibration times, as described below.

Quartz Geothermometer: The solubility of quartz in water is a strong function of temperature, and thus the concentration of silicic acid in a fluid sample can be related to an underground fluid temperature. Rimstidt (1979) compiled the available equilibrium data and obtained the following correlation:

$$C^{\infty} = 6\times10^{4} \times 10^{(1.881-2.028\times10^{-3}T-1560/T)} \quad (6)$$

where C^{∞} is the equilibrium solubility (in ppm) and T the absolute temperature (in K).

The main question of the applicability of this relation resides in the assumption of equilibrium. If injected fluid does not stay in the reservoir long enough to reach equilibrium, erroneously low geothermometer readings will result. The kinetics of quartz dissolution has been studied by many workers (Kitahara, 1960, Van Lier et al., 1960, Siebert et al., 1963, Weill and Fyfe, 1964, Stober, 1967, and Rimstidt, 1979), and the results were reviewed and further experiments performed by Robinson (1982). The accepted rate law in a closed vessel is:

$$\frac{dC}{dt} = ka^*(C^{\infty} - C) \quad (7)$$

where k is the dissolution rate constant (in m/sec) and a* the rock surface area to fluid volume ratio (m^{-1}). Thus $1/ka^*$ is a characteristic reaction time, and equilibrium may be safely assumed for downhole fluid residence time greater than three times this reaction time, or $\tau_r > 3/ka^*$. In a fractured

reservoir, a* = 2/b, where b is the average fracture aperture. In reality the fraction of rock which is quartz should also be included, but for this approximate calculation this correction is unnecessary. The rate constant k was found by Robinson (1982) to obey an Arrhenius temperature dependence with E_a = 78.3 kJ/mol and A_r = 2.712 m/sec. Thus the criterion for equilibration of the quartz geothermometer is

$$\tau_r > 1.5\times10^{-4}\ b(e^{9418/T}) \qquad (8)$$

where τ_r is in hours, b in m, and T in K. Equation (8) should always be used to evaluate the likelihood of chemical equilibium of the quartz geothermometer, as a lack of equilibrium will result in erroneously low temperatures. A typical average fracture aperture for HDR reservoirs is on the order of 10^{-3} m (1 mm). Using this value, the approximate equilibration times for flow in hyraulically stimulated fractures at 150, 200, and 250°C are 690 hr, 66 hr, and 10 hr respectively. In the fracturing experiments analyzed here, the downhole residence times are long enough and temperatures high enough for equilibration. Note however that in geothermal systems of intermediate temperature (150-200°C) the quartz geothermometer must be used with caution when evaluating the geochemistry of injection-flow experiments of limited duration.

Other potential problems with the quartz geothermometer are polymerization or deposition of silica, mixing of fluids of different temperatures, and flashing during sample collection. In general, the quartz geothermometer is not affected strongly by deposition unless long residence times at large degrees of supersaturation are encountered, such as in an above ground heat exchanger or in an injection well. As a result, if a fluid equilibrates with respect to quartz at one temperature and then encounters a section of reservoir at a lower temperature, the geothermometer reading at the higher temperature is preserved. Fluid dilution and mixing will obviously affect the reading, although reequilibration after mixing can in many cases eliminate the problem. Flashing of steam will result in a higher concentration in the remaining fluid sample, but this effect can be accounted for precisely by calculating the steam fraction using an enthalpy balance.

Na-K-Ca Geothermometer: This geothermometer provides a measure of rock temperature through the ratios of these ions in solution, which are controlled by cation exchange reactions among the feldspars and feldspar alteration minerals (Fournier and Truesdell, 1973). The empirical relationship proposed by Fournier and Truesdell is

$$T = \frac{1647}{\log_{10}(Na/K)+\beta[\log_{10}(\sqrt{Ca}/Na)+2.06]+2.47} \qquad (9)$$

where concentrations are in ppm, T in K, and β = 1/3 for T > 100°C and 4/3 for T < 100°C. The major difference of this geothermometer from the quartz measurement is that the dissolution/alteration reactions require much longer times for equilibrium. Thus only fluid present in the reservoir for long periods of time will reflect the downhole temperature, and injected fluid will not reach equilibrium in a typical short term flow test. Nonetheless, the effects of dilution caused by injection of clean fluid are not great since the ratios of ions in solution are used in Equation (9). As long as the fluid samples contain some of the reservoir pore fluid, the geothermometer will provide a good measure of downhole temperature. Mixing of fluids of somewhat different temperatures will affect the reading, with the measured result falling in between the temperatures of the fluids before mixing.

Experiment 2032: In this fracture experiment which resulted in the microseismic events shown in Figure 3, equipment failure resulted in an uncontrolled vent back up the injection wellbore after pumping 21000 m^3 of fluid. After 34 hours of venting the situation became safe enough to collect several fluid samples. Table 1 shows the quartz and Na-K-Ca geothermometer readings of these samples. Since flashing occured during the vent, the quartz geothermometer readings using the simple equilibrium relationship are artificially high. Grigsby and Matsunaga (1984) have corrected these values for the conditions at Fenton Hill (where the boiling point of water is 90°C) and obtained an average value of 216°C. Both geothermometers give a temperature of about 215°C, which is approximately equal to the initial rock temperature at the injection depth during this experiment. This suggests that the injected fluid traveled away from the injection region with no tendency to flow preferentially either upward or downward. The seismic event locations (Figure 3) agree with this conclusion. Although this may not seem surprising, a later experiment described below (Experiment 2061) resulted in a different conclusion, and the geochemistry evaluation added to the interpretation of the test.

Experiment 2059: This test was the first to result in interwell flow, and the geochemical measurements in this case were of produced fluid rather than water being vented back up the injection well. The first few samples were simply fluid residing in the production well and not indicative of reservoir chemical conditions. Once this fluid was displaced, the Na-K-Ca concentrations listed in Table 1 indicate a fluid temperature of 240-250°C. This range agrees with the initial rock

temperature at the known injection region, determined precisely from a temperature log performed after the experiment. The fluid apparently short-circuited directly from one well to the other, and showed no tendency to take a more circuitous route downward before reaching the production well. If it had traveled downward, higher geothermometer measurements would have been obtained. The decline in the geothermometer temperatures during the experiment are probably due to fluid mixing which occured during the experiment. These effects are difficult to discern with the geothermometers, which smear the actual downhole temperatures into an average temperature.

Experiment 2061: During this unsuccessful attempt to create more fracture flow connections between the wells, samples of the ventback fluid were collected. The quartz and Na-K-Ca geothermometers do not agree in this case. We believe that dilution and mixing probably affected the Na-K-Ca readings and that the quartz values are more representative of the reservoir fluid. The values of the quartz geothermometer (277 and 286°C) are much higher than the rock temperature at the injection region, indicating that the vented fluid was being recovered from a region much deeper than the injection depth. Since the target depth in the production well was above the injection zone but the water traveled preferentially downward, it is not surprising that the desired flow connection was not achieved. This explanation agrees with microseismic event locations during this experiment, which clustered far below the injection region. The geochemical evidence cited here augments that finding and provides a more complete picture of the downhole flow geometry at remote locations away from the injection wellbore.

Experiment 2062: This experiment, like Experiment 2059, resulted in an interwell connection, and the samples collected were production fluid samples. The geothermometer data were quite similar to the previous test, with downhole temperatures close to that of the rock near the injection region. Once again the injected fluid swept pore fluid from this depth to the production well, and the geothermometer readings reflect the temperature of the rock at this depth.

In summary, the geothermometer measurements can provide additional information about reservoir geometry during a hydraulic fracturing experiment. Specifically, the depths at which fluid resided when in the reservoir, and hence the flow direction (e.g. upward or downward) can be determined from geochemical analyses, knowing the initial rock temperature as a function of depth from a background temperature survey. In the experiments described above, this geochemical information agreed well with microseismic event locations, which indicate where the fluid is traveling in space. This suggests that in pumping experiments in which no microseismicity is induced, geothermometer readings can be used to determine the location of fluid flow paths (in the vertical direction). In one such interwell flow experiment performed recently at Fenton Hill (Brown, 1985) there was no microseismicity, and a temperature log indicated two possible depths for fluid entering the wellbore. The geochemical evidence ruled out the shallower of the two entrance depths, and the flow geometry was thus determined.

CONCLUSIONS

The Fenton Hill field tests have identified several practical conclusions regarding the use of tracers and geochemistry during hydraulic fracturing experiments.

1. Tracer and geochemical information must be interpreted differently during hydraulic fracturing due to unequal inlet and outlet flow rates and transient effects.
2. Two simple models of flow in main fractures with water storage in secondary joints were developed. These models allow the volume of the main fracture flow paths to be estimated from an interwell test.
3. During hydraulic fracturing tests, tracer should be injected only after flow communication has been established between the wells.
4. The quartz and Na-K-Ca geothermometers are useful to identify the downhole temperature and hence depth at which fluid is traveling.
5. The quartz geothermometer equilibrates rapidly enough in fractured reservoirs at 250°C to be used accurately. An approximate criterion has been developed to evaluate the likelihood of equilibration.
6. The Na-K-Ca geothermometer does not equilibrate rapidly, but still may be used in injection-flow experiments because sufficient quantities of indigenous pore fluid are contained in the fluid samples. It is somewhat more susceptible to problems due to fluid mixing and dilution, however.

ACKNOWLEDGEMENTS

This work was funded by the U. S. Department of Energy. Field data were collected and analyzed primarily by Pat Trujillo and Dale Counce, with help from Ron Aguilar, Chuck Grigsby, and George Cocks.

NOMENCLATURE

$\dot{a}$	rock surface area to fluid volume ratio (m^{-1})
A_r	reaction rate pre-exponential factor (m/sec)
b	fracture aperture width (m)
C	dissolved silica concentration (ppm)
C^{∞}	equilibrium solubility of quartz (ppm)

E_a	reaction rate activation energy (kJ/mol)
k	quartz dissolution reaction rate constant (m/sec)
Q	volumetric flow rate (m^3/sec)
Q_{in}	inlet volumetric flow rate (m^3/sec)
Q_{out}	outlet volumetric flow rate (m^3/sec)
T	temperature (K)
V_f	fracture volume (m^3)
V_m	modal volume (m^3)
τ	modal residence time (sec)
τ_r	characteristic reaction time for quartz dissolution (sec)

REFERENCES

Brown, D. W. (1985), "Analysis of the EE-3A Temperature Logs Following the Experiment 2064 Pre-Pump," Los Alamos National Laboratory ESS Division Internal Memorandum, Dec. 24, 1985.

Fournier, R. O. and A. H. Truesdell (1973), "An Empirical Na-K-Ca Geothermometer for Natural Waters," Geochim. et Cosmochim. Acta, 37, 1255-1275.

Grigsby, C. O. (1983), "Rock-Water Interactions in Hot Dry Rock Geothermal Systems: Reservoir Simulation and Modeling," S. M. Thesis, Massachusetts Institute of Technology Department of Chemical Engineering.

Grigsby, C. O. and I. Matsunaga (1984) in Murphy, H. D. (ed), "Experiment 2032 Report," Los Alamos National Laboratory ESS Division Internal Memorandum, ESS-4-70-84, March 26, 1984.

House, L., H. Keppler and H. Kaieda (1985), "Seismic Studies of a Massive Hydraulic Fracturing Experiment," Transactions Geothermal Resources Council, Vol 9 - Part II, paper presented at 1985 Geothermal Resources Council annual meeting, Honolulu, Hawaii.

Kitahara, S. (1960), "The Solubility Equilibrium and the Rate of Solution of Quartz in Water at High Temperatures and High Pressures," Rev. Phys. Chem. Japan, 30, 2, 122-130.

Rimstidt, J. D. (1979), "Kinetics of Silica-Water Reactions," PhD Thesis, The Pennsylvania State University Department of Geosciences.

Robinson, B. A. (1982), "Quartz Dissolution and Silica Deposition in Hot Dry Rock Geothermal Systems," S. M. Thesis, Massachusetts Institute of Technology Department of Chemical Engineering.

Robinson, B. A. and J. W. Tester (1984), "Dispersed Fluid Flow in Fractured Reservoirs: An Analysis of Tracer-Determined Residence Time Distributions," J. Geophys. Res., 89, B12, 10374-10384.

Siebert, H., W. V. Youdelis, J. Leja and E. O. Lilge (1963), "The Kinetics of the Dissolution of Crystalline Quartz in Water at High Temperatures and High Pressures," Unit Processes in Hydrometallurgy, The Metallurgical Society of A.I.M.E. Conference, 24, 284-299.

Stober, W. (1967), "Formation of Silicic Acid in Aqueous Suspensions of Different Silica Modifications," Equilibrium Concepts in Natural Water Systems, American Chemical Society, 67, 161-182.

Tester, J. W., R. L. Bivins and R. M. Potter (1982), "Interwell Tracer Analyses of a Hydraulically Fractured Granitic Geothermal Reservoir," Soc. Pet. Eng. J., 22, 537-554.

Van Lier, J. A., P. L. de Bruyn and J. Th. G. Overbeek (1960), "The Solubility of Quartz," J. Phys. Chem., 64, 1675-1682.

Weill, D. F. and W. S. Fyfe (1964), "The Solubility of Quartz in H_2O in the Range 100-4000 Bars and 400-550°C," Geochim. et Cosmochim. Acta, 28, 1243-1255.

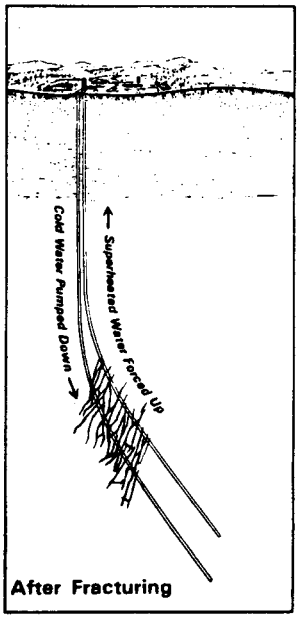

Figure 1. Hot Dry Rock Geothermal Concept

TABLE 1
CHEMICAL CONCENTRATIONS AND GEOTHERMOMETER RESULTS

EXPERIMENT	DATE	TIME	Na	K	Ca	SiO_2	GEOTHERMOMETER TEMPERATURES (°C) Na-K-Ca	Quartz
2032*	12/10/83	15:30	900	100	52.4	380	210	240
	12/11/83	15:30	1310	142	43.3	440	218	258
	12/12/83	10:30	1360	154	98	415	213	251
		13:30	1410	164	93	430	216	255
		16:15	1480	167	80.3	438	216	257
	12/14/84	09:30	1410	157	129	417	210	251
		16:00	1480	167	138	420	211	252
2059	5/28/85	02:15	1220	98	14		209	
		03:30	1630	175	65		217	
		04:20	2860	468	174		247	
		05:00	2770	414	113		245	
		05:30	2750	411	115		245	
		06:00	2430	354	93		243	
		07:00	2010	316	72		247	
		09:00	1900	283	55		245	
		10:00	1360	181	40		233	
		11:00	1350	221	59		242	
		13:00	1160	175	58		233	
		16:00	1320	177	38		233	
		20:00	1425	192	42		234	
	5/29/85	02:00	1340	182	35		235	
		08:00	1400	180	36		232	
		15:00	1360	176	38		232	
2061	7/2/85	10:00	2010	280	47	510	243	277
		17:00	2010	283	50	542	243	286
2062	7/18/85	17:00	1720	220	232	410	216	249
		18:45	2250	350	148	430	240	255
		19:00	2010	292	107		237	
		20:00	1920	318	108		244	
		21:30	1900	265	77		236	
		22:45	1560	239	62		241	
	7/19/85	00:30	1670	219	55		233	
		03:00	1270	184	50		235	

*Quartz geothermometer values not corrected for flashing.

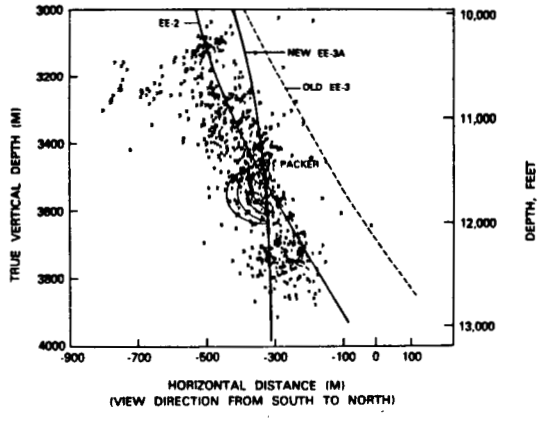

Figure 3. Elevation View of Phase II Wellbores and Experiment 2032 Microseismicity

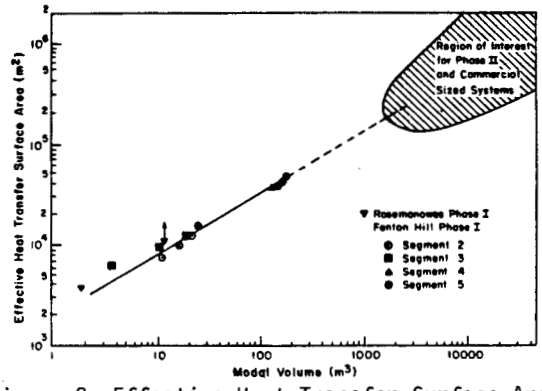

Figure 2. Effective Heat Transfer Surface Area Versus Modal Volume Correlation

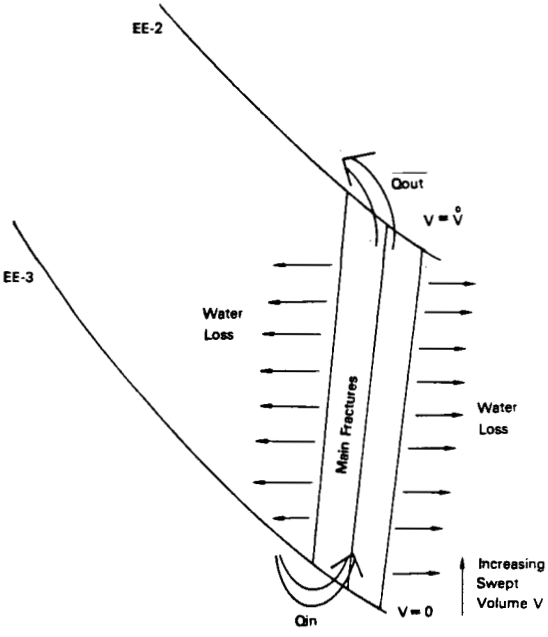

Figure 4. Schematic of Fracture Flow, Water Loss Model

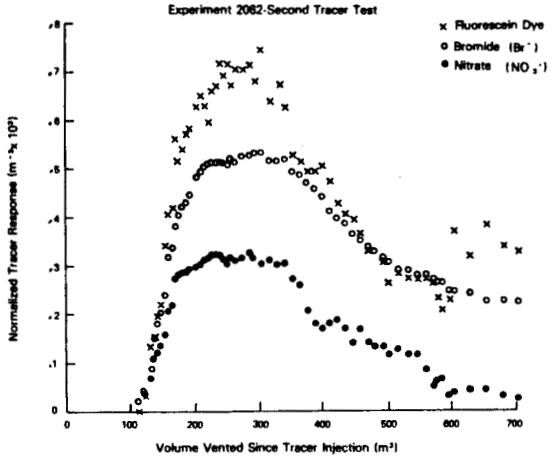

Figure 5. Normalized Tracer Response Curves for 2nd Tracer Test of Experiment 2062

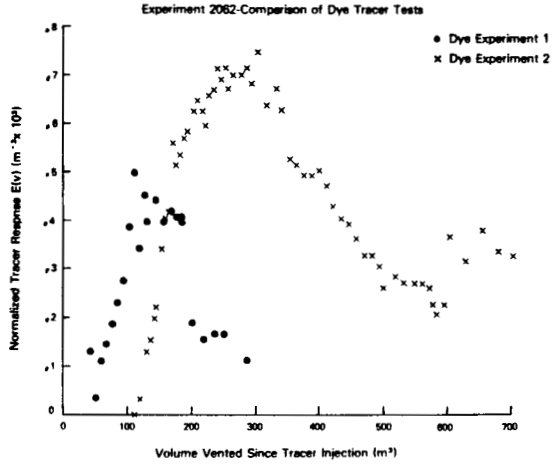

Figure 6. Comparison of Tracer Response Curves for the 1st and 2nd Tracer Tests of Experiment 2062